Journal of Hydrology 523 (2015) 822–829

Contents lists available at ScienceDirect

Journal of Hydrology

journal homepage: www.elsevier.com/locate/jhydrol

Deforestation offsets water balance changes due to climate variability in the Xingu River in eastern Amazonia

Prajjwal K. Panday [a,*], Michael T. Coe [a], Marcia N. Macedo [a], Paul Lefebvre [a], Andrea D. de Almeida Castanho [a,b]

[a] Woods Hole Research Center, Falmouth, MA, USA
[b] Federal University of Ceará, Fortaleza, Brazil

ARTICLE INFO

Article history:
Received 4 December 2014
Received in revised form 3 February 2015
Accepted 7 February 2015
Available online 16 February 2015
This manuscript was handled by Konstantine P. Georgakakos, Editor-in-Chief, with the assistance of Matthew Rodell, Associate Editor

Keywords:
Amazon
Deforestation
Hydrology
Numerical modeling
Water balance
Xingu River Basin

SUMMARY

Deforestation reduced forest cover in Brazil's Xingu River Basin (XB; area: 510,000 km^2) from 90% of the basin in the 1970s to 75% in the 2000s. Such large-scale land cover changes can substantially alter regional water budgets, but their influence can be difficult to isolate from that of natural climate variability. In this study, we estimate changes to the XB water balance from the 1970s to the 2000s due to climate variations and deforestation, using a combination of long-term observations of rainfall and discharge; satellite-based estimates of evapotranspiration (MODIS) and surface water storage (GRACE); and numerical modeling estimates (IBIS) of water budget components (evapotranspiration, soil moisture, and discharge). Model simulations over this period suggest that climate variations alone accounted for a −82 mm decrease (mean per unit area) in annual discharge (−14%, from 8190 m^3 s^{-1} to 7806 m^3 s^{-1}), due to a −2% decrease in precipitation and +3% increase in evapotranspiration. Deforestation alone caused a +34 mm increase in annual discharge (+6%), as a result of a −3% decrease in evapotranspiration and +1% increase in soil moisture across the XB. Climate variability and land cover change thus had opposite effects on the XB water balance, with climate effects masking deforestation-induced changes to the water budget. Protected areas, which cover 55% of the basin, have helped to mitigate the effects of past deforestation on water recycling in the Xingu. However, our results suggest that continued deforestation outside protected areas could trigger changes of sufficient magnitude to offset climate variability.

1. Introduction

Large-scale deforestation in the states of Mato Grosso and Pará in the eastern Brazilian Amazon first began in the 1970s, facilitated by federal government colonization programs that supported massive infrastructure development, and continued in the 2000s due to growing markets for export-oriented agricultural commodities (Barona et al., 2010; DeFries et al., 2013). Deforestation in the region began with clearing of forests for pasturelands, encouraged by generous fiscal incentives for large-scale cattle ranching (Nepstad et al., 2006). Pasture remains the predominant land use following deforestation today, although commodity crops such as soybeans and maize are expanding rapidly – driven by the growing influence of global markets on the Amazonian economy and facilitated by relatively low land prices and improved transportation infrastructure (Macedo et al., 2012; Neill et al., 2013; Nepstad et al., 2006). The states in the Amazon's deforestation frontier (i.e. Mato Grosso, Pará, and Rondônia) accounted for 85% of all Amazon deforestation from 1996 to 2005 (Nepstad et al., 2009). From 2006 to 2010 annual deforestation declined dramatically, particularly in Mato Grosso where it decreased to 30% of its historical (1996–2005) average (Macedo et al., 2012).

Despite reductions in deforestation rates, the eastern Amazon region – a transition zone between rainforest and savanna environments – remains particularly vulnerable to climate changes associated with feedbacks from ongoing land use change (Coe et al., 2013). The expansion and intensification of agriculture over tropical forests fundamentally shifts how incoming precipitation and radiation are partitioned among sensible and latent heat fluxes and runoff (Bonan, 2008; Coe et al., 2013; Foley et al., 2005; Neill et al., 2013; Silvério, submitted). Relative to the forests they replace, crops and pasture grasses have reduced root density and depth, and lower leaf area index (LAI), resulting in decreased water demand and lower evapotranspiration (Coe et al., 2009, 2013; Costa et al., 2003; D'Almeida et al., 2007; De Moraes et al., 2006; Lathuillière et al., 2012; Nepstad et al., 1994; Pongratz et al., 2006; Scanlon et al., 2007; Silvério, submitted). At local and regional scales (i.e. watersheds of 10 s to 100,000 s of km^2), such

* Corresponding author at: Woods Hole Research Center, 149 Woods Hole Road, Falmouth, MA 02540, USA. Tel.: +1 (508) 444 1545; fax: +1 (508) 444 1845.
E-mail address: ppanday@whrc.org (P.K. Panday).

http://dx.doi.org/10.1016/j.jhydrol.2015.02.018
0022-1694/

reductions in evapotranspiration lead to increased soil moisture and discharge (Coe et al., 2011, 2009; Hayhoe et al., 2011; Neill et al., 2006). At continental scales (i.e. Amazon Basin) these land cover changes may feedback on regional climate by reducing rainfall and decreasing discharge (D'Almeida et al., 2007; Davidson et al., 2012; Stickler et al., 2013).

Changes in the water balance operate across multiple spatial and temporal scales and the effect of land cover and land use changes can be difficult to isolate from background climate variability (Costa et al., 2003). Studies documenting changes in discharge and water yield (precipitation minus evapotranspiration per unit area) as a function of land cover change are abundant for small watersheds (<10 km^2) (Bosch and Hewlett, 1982; Hodnett et al., 1995; Williams and Melack, 1997), but few studies have evaluated these effects in meso- or large-scale river basins in the Amazon (but see Coe et al., 2011, 2009; Costa et al., 2003). To address this gap, we quantify the independent effects of historical land cover change and climate on the water balance of the Xingu Basin (XB, Fig. 1), the fourth largest subwatershed of the Amazon.

The XB originates in the Brazilian Cerrado (woodlands–savannas), flowing northward through the transitional forests of the Mato Grosso plateau and the dense rainforests of Pará before reaching the Amazon River (Fig. 1). Of the 510,000 km^2 basin area, approximately 200,000 km^2 is protected as indigenous lands and 80,000 km^2 as nature reserves (Schwartzman et al., 2013). Mean decadal forest cover in the XB decreased from 90% in the 1970s to 75% in the 2000s. Of the 100,000 km^2 deforested in the XB by 2010, 91% occurred outside protected areas – much of it concentrated in the upper Xingu Basin in the state of Mato Grosso, which experienced among the highest deforestation rates in Brazil from 1995 to 2005 (Macedo et al., 2013; Schwartzman et al., 2013).

To estimate the impacts of land cover change and climate variability on the water budget of the XB, we used a diverse set of observational and modeling tools, including long-term observations of

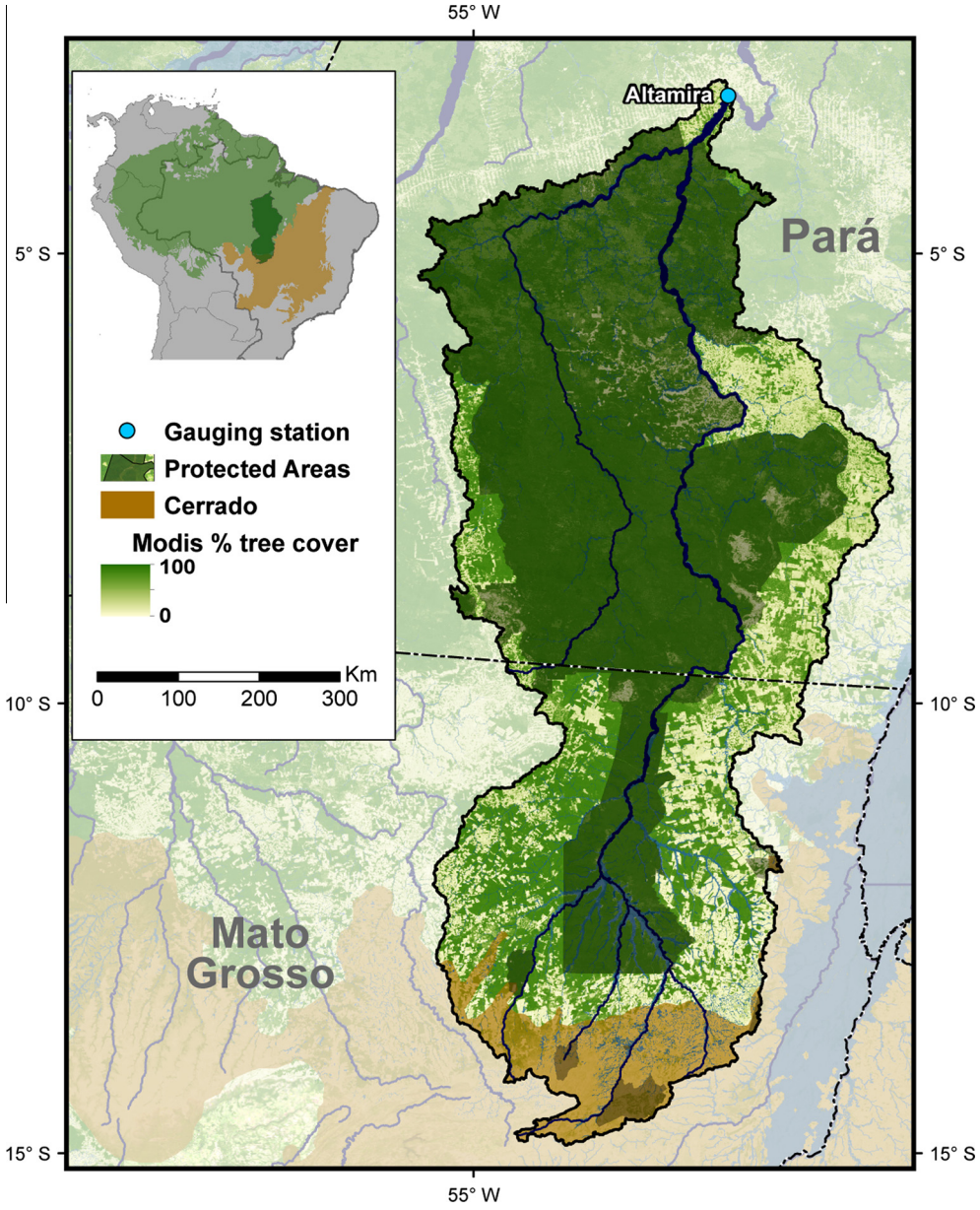

Fig. 1. Study area showing Xingu River Basin with land cover as of 2000. Inset figure shows the Xingu Basin in the context of forest and savannah biomes.

rainfall and discharge; satellite-based estimates of evapotranspiration (MODIS; Moderate Resolution Imaging Spectroradiometer) and surface water storage (GRACE; Gravity Recovery and Climate Experiment); and numerical modeling (IBIS; Integrated BIosphere Simulator) of key components of the water balance (i.e. evapotranspiration, soil moisture, and discharge). Here we use a water budget approach to evaluate the major fluxes (evapotranspiration and total runoff) and storage changes (soil water storage) in the Xingu Basin since the 1970s as an individual and combined function of deforestation and climate variability.

2. Methodology

2.1. Numerical modeling of hydrological budget

Using the dynamic vegetation model IBIS, we ran a series of simulations to estimate the XB water budget and quantify the relative contributions of historical land cover change and climate variation to each component of the water budget. IBIS integrates various terrestrial ecosystem processes (i.e. energy, water, and momentum exchange among soil, vegetation, and atmosphere), canopy physiology, vegetation phenology, and long-term ecosystem dynamics within a single, physically consistent model (Foley et al., 1996; Kucharik et al., 2000). Land surface processes are represented by two vegetation layers (woody and herbaceous) and six soil layers (extending from the surface to a depth of 8 m), which simulate moisture dynamics based on the Richards equation. The model has a root-water-uptake module that considers water stress compensation, based on an asymptotic root distribution function, and a surface soil water infiltration rate, based on the Green–Ampt formulation (Li et al., 2006). Surface runoff is simulated as the difference between rainfall landing on the surface and soil infiltration, whereas sub-surface runoff is water in excess of that used by plants during photosynthesis. We ran IBIS at $0.5^\circ \times 0.5^\circ$ horizontal resolution with a 1-h time step from 1940 to 2011, using the Climate Research Unit (CRU TS, v.3.21) climate data. To simulate the water balance without deforestation, we used a potential vegetation map from Ramankutty and Foley (1998), which represents the vegetation that would be present without human intervention.

This study follows an experimental design previously used by Coe et al. (2009) and Stickler et al. (2013) to estimate the impacts of land cover change on streamflow in Amazonian watersheds. To isolate the influence of historical land use change on each component of the XB water balance, we ran two sets of IBIS simulations using identical climate inputs: (1) a scenario with potential vegetation (RUN-POT), as depicted by Ramankutty and Foley (1998), and (2) a scenario where all vegetation is replaced by C_4 grasses (RUN-GRASS), representing complete deforestation of the XB. We then used annual MODIS land cover data (MCD12Q1) for the 2001–2010 period to linearly mix evapotranspiration, soil moisture, and runoff (surface and subsurface), simulated by IBIS at a monthly time step. For instance, we calculated total runoff from 2001 to 2010 as the sum of runoff values from RUN-POT and RUN-GRASS over the undisturbed and disturbed fractions of a given grid cell as follows.

$$R_t = F_f \times R_p + (1 - F_f) \times R_g \quad (1)$$

where F_f is the forested fraction from the MODIS land cover maps, R_p is the total runoff from RUN-POT and R_g is the total runoff from RUN-GRASS. For an undisturbed pixel ($F_f = 1$), the runoff comes entirely from the RUN-POT simulation. This linear mixing of simulated results approximates the linear averaging of land cover types occurring within each IBIS grid cell. This new set of hydrological outputs for the 2000s is referred to as the RUN-LUC simulation. Another set of hydrological outputs for 2001–2010, referred to as RUN-01, was also created by linearly mixing the IBIS outputs and holding land cover constant to the MODIS 2001 period. The difference between RUN-LUC and RUN-01 provides a measure of the effects of land cover change during the MODIS observational period.

In this study, we assess the total water balance of a watershed as the balance between inputs, losses, and changes in storage as follows.

$$P = \mathrm{ET} + \frac{\delta S}{\delta t} + R \quad (2)$$

where P is precipitation, R is the total basin discharge, ET is evapotranspiration, and δS is the change in soil water storage. For consistency among model simulations and satellite-derived measurements, we used a one-month time step (δt). In addition to the monthly change in soil moisture, we analyzed simulated monthly average soil moisture to examine the total amount of subsurface water storage. Decadal-mean monthly averages of the hydrologic components were created using 10 water-years (120 months), where the water year was defined as the 12 month period beginning in October and ending in September of the following year (e.g. water-year 2000 encompasses October 1999 to September 2000).

2.2. Model validation

We validated each of the hydrologic components derived from IBIS for the 2000s, using satellite-based estimates for ET and $\delta S/\delta t$ and observed (1971–2010) streamflow data for the XB at Altamira (Fig. 1, 3°15′S, 52°10′W), obtained from the Brazilian National Water Agency (ANA, http://hidroweb.ana.gov.br/).

To validate the IBIS ET estimates for the XB, we compared them to the MODIS (MOD16A2) monthly evapotranspiration (hereafter MOD16ET) dataset (Mu et al., 2011). MOD16ET is a global ET product, estimated based on the Penman–Monteith equation, using daily meteorological data from NASA's Global Modeling and Assimilation Office (GMAO) reanalysis dataset and 8-day remotely-sensed vegetation property dynamics from MODIS (land cover, albedo, leaf area index, and Enhanced Vegetation Index) as inputs. MOD16ET is available from 2000 to 2013 at 1 km^2 horizontal resolution for the entire global vegetated land surface at 8-day and monthly time intervals. The ET algorithm considers both the surface energy partitioning process and environmental constraints on ET (Mu et al., 2007). Uncertainties in the MOD16ET data stem from uncertainty in the input data, including biases in the GMAO meteorology data, uncertainties in MODIS-derived inputs, limitations of the algorithm in representing biophysical processes, and uncertainty of biophysical and environmental parameters.

To independently validate the IBIS water storage simulations, we used the GRACE satellite total water storage anomaly product. Since its launch in mid-2002, GRACE has provided estimates of total water storage anomalies (TWS), which is the total vertically-integrated water present above and beneath the surface of the Earth, with a resolution of a few hundred kilometers (Rodell et al., 2004; Swenson et al., 2003). The GRACE satellite observes temporal variations of Earth's gravitational potential using twin satellites. Variations in TWS on land and in the ocean can be inferred from changes in the gravitational field associated with changes in mass. Several post-processing filtering approaches are used to dampen the errors in TWS estimates, which arise from signal degradation that can modify the geophysical signal of interest (Landerer and Swenson, 2012). Several studies have used GRACE data to study interannual to decadal variability in TWS, and the state of hydrological stress in the Amazon River basin (Chen et al., 2009; Crowley et al., 2008; de Linage et al., 2013; Pokhrel et al., 2013). GRACE TWS estimates also provide a set of indepen-

dent data to constrain and evaluate TWS from global land surface models. In this study, we use the RL05 version of GRACE data, with a spatial resolution of $1^\circ \times 1^\circ$ for the 2004–2012 time period (Landerer and Swenson, 2012) [available at http://grace.jpl.nasa.gov/data/gracemonthly/massgridsland/]. Monthly changes were computed from GRACE TWS anomalies, which were compared against average monthly simulated soil moisture anomalies from IBIS for the same years.

Finally, we performed a validation based on comparisons of the following three monthly water balance calculations for the XB: (a) the difference between monthly precipitation from CRU data and monthly MOD16ET ($P - ET_{MODIS}$), (b) the difference between monthly CRU precipitation and monthly IBIS evapotranspiration ($P - ET_{IBIS}$), and (c) the monthly simulated runoff from RUN-POT (R_{IBIS}), which is mathematically equivalent to the CRU precipitation minus IBIS simulated ET and the change in monthly soil moisture ($P - ET_{IBIS} - \delta S/\delta t$). We then compared the modeled water balances and simulated discharge against observed annual discharge at Altamira from 2001 to 2010.

2.3. Partitioning the impacts of climate and land cover

We used an analytical approach similar to that of Costa et al. (2003) and Coe et al. (2011) to estimate the relative influences of land cover change and climate variability on XB hydrology. First we compared decadal means of the observed and modeled hydrologic components for the 1970s and 2000s. Decadal means were averaged across water-years for each water budget component and used to develop monthly and annual mean values for each of the two decades. Monthly values of precipitation from CRU data were spatially averaged over the XB and summed across each water-year to estimate annual mean precipitation. Similarly, monthly mean values of observed discharge at Altamira were used to compute annual and decadal average discharge. Because the observed discharge time series begins in January 1971, the 1970s decadal mean was calculated based on only 108 months (1972–1980), compared to 120 months for the 2000s (2001–2010).

First, we compared the simulated decadal mean hydrological budgets for the 1970s and 2000s with and without land cover changes (Table 1). To estimate the water budget of the XB as a function of climate variability alone, we used the RUN-POT simulations to compute decadal mean values of simulated ET, δS, R, and average soil moisture for the 1970s and 2000s. Decadal mean values of the water budget components for the 2000s from the RUN-LUC simulation incorporated the climate variations and land cover distribution of the 2000s from MODIS. The difference between the water budget components from the RUN-POT and RUN-LUC simulations for the 2000s removes the climate signal and isolates the effect of land cover changes over that period. Second, we examined changes in the water balance due to land cover changes from 2001 to 2010 at finer temporal resolution. The availability of annual MODIS land cover maps for the 2000s allowed estimation of the cumulative changes in water balance components due to land use transitions during that period. Differences in the water budget components for the RUN-LUC and RUN-01 simulations can be attributed to land cover alone, since climate inputs were identical for the two simulations.

3. Results

3.1. Hydrological balance from 2001 to 2010

3.1.1. Annual mean

The decadal mean water balance components of the RUN-LUC simulation (Table 1), which explicitly includes deforestation, compare well with satellite-derived and field-based estimates. The mean simulated ET for the 10-year period is 1490 mm yr^{-1}, which is 73% of the observed decadal mean precipitation (P, 2048 mm yr^{-1}) used as an input to IBIS (Table 1). The decadal mean change in water storage (δS) is close to zero, as expected for a long-term climatic average. Simulated discharge is 558 mm yr^{-1} (8190 m^3 s^{-1}), which is within 5% of the observed value of 540 mm yr^{-1} (7806 m^3 s^{-1}), thereby closing the water budget (Eq. (2)) for the XB. A simple estimate of ET (ET = P–R–δS), using observed values for each term and assuming negligible water storage changes, yields a value of 1508 mm yr^{-1} (Table 1), which is within 3% of the IBIS simulated ET. The MODIS-derived estimate of ET is 1236 mm yr^{-1}, about 20% less than the ET simulated by IBIS and inferred from the simple water budget analysis. The MODIS-derived product likely underestimates ET due to uncertainties associated with the algorithm and input datasets.

Table 1
Long term mean of hydrological variables in the Xingu River Basin upstream of Altamira. Percent forest is the fraction of basin in forest. Decadal mean annual discharge (R) and percent change for the 1970s and 2000s for: (1) observed discharge for Xingu at Altamira (OBS); (2) simulated in RUN-POT with the climate of the 1970s and 2000s but with fixed potential vegetation; and (3) simulated in RUN-LUC with 2000s climate linearly mixed using MODIS land cover. Percent relative error (%RE) of the simulated decadal mean discharge of RUN-POT and RUN-LUC compared to the observed discharge. Pearson product moment correlation coefficient (r) between the 12 decadal mean monthly values of simulated discharge and 12 monthly observed values. Decadal mean annual observed precipitation (P) in mm yr^{-1} for each decade and percent change. Evapotranspiration (ET) for each decade calculated as the difference between precipitation and discharge for the observations (OBS), RUN-POT, and RUN-LUC. Decadal mean of simulated change in soil storage (δS) and average soil moisture for (S) RUN-POT and RUN-LUC. All RUN-LUC differences are computed as the difference between RUN-LUC in the 2000s and RUN-POT in the 1970s.

Xingu		1970s	2000s	% Change
% Forest		90	75	−15%
R mm yr^{-1}	OBS	576	540	−6%
	RUN-POT	606	524	−14%
	RUN-LUC		558	−8%
%RE	RUN-POT	−5%	3%	
	RUN-LUC		−3%	
r	RUN-POT	0.95	0.89	
	RUN-LUC		0.90	
P mm yr^{-1}	OBS	2096	2048	−2%
ET mm yr^{-1}	OBS	1520	1508	−1%
	MODIS		1236	
	RUN-POT	1480	1524	3%
	RUN-LUC		1490	1%
δS mm yr^{-1}	RUN-POT	−1	−2	–
	RUN-LUC		−3	–
S mm yr^{-1}	RUN-POT	2403	2374	−1%
	RUN-LUC		2389	−1%

3.1.2. Monthly mean

Observed precipitation is highly seasonal, peaking at over 300 mm month^{-1} in February–March and diminishing to less than 50 mm month^{-1} in June–August (Fig. 2a). Land surface processes, associated primarily with vegetation, mediate the conversion of precipitation into ET, δS and R. As expected, ET in the XB is correlated with P ($r = 0.77$, $n = 12$) but exhibits much lower seasonal variability, given the predominance of evergreen vegetation, which evapotranspires at high rates as long as there is soil moisture available. Mean simulated ET for the wet season (November–April) is 134 mm month^{-1}, about 17% higher than the dry season ET (May–October) of 115 mm month^{-1}. The ET/P ratio is larger during the months of May–September and exceeds 1 during the dry season. Simulated ET peaks in February–March at nearly 140 mm month^{-1} and decreases to slightly less than 100 mm month^{-1} at the end of the dry season (September).

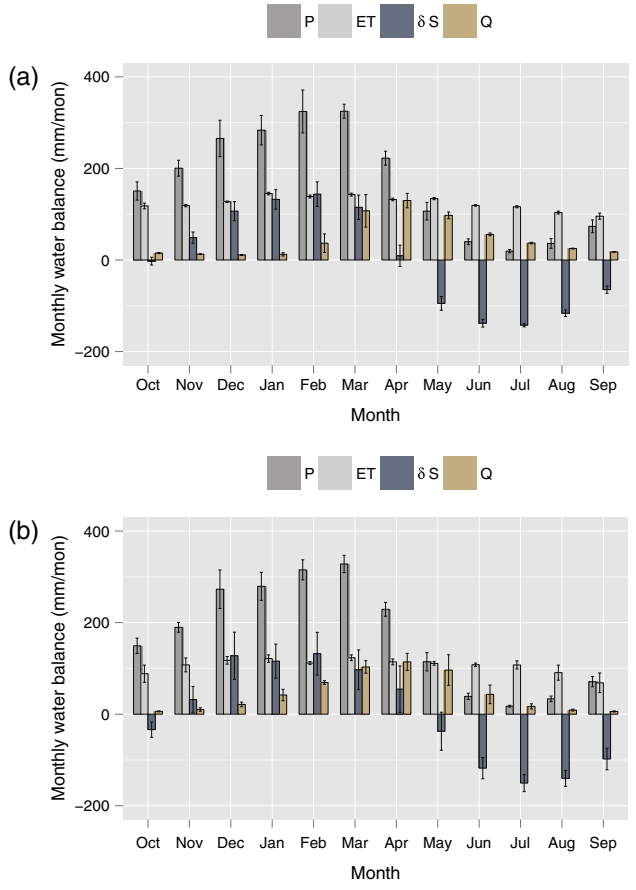

Fig. 2. (a) Average monthly mean components of the simulated water budget in the Xingu River Basin for 2001–2010. Precipitation (P, Climate Research Unit – v.3.21), evapotranspiration (ET), change in soil moisture storage (δS), and total runoff (R). Observed P is used as input to drive the IBIS simulations. ET, δS, and R are subsequently simulated by IBIS (RUN-LUC). Vertical bars are the standard deviation from the mean; and (b) average monthly mean components of the observed water budget in the Xingu River Basin for 2004–2010 where P is precipitation (CRU), ET is MODIS derived evapotranspiration (MOD16ET), δS is change in terrestrial water storage from GRACE, and R is observed discharge at the Altamira station on the Xingu (Fig. 1). Vertical bars are the standard deviation from the mean.

Simulated changes in soil moisture storage are also strongly correlated with precipitation ($r = 0.98$, $n = 12$). Soil moisture recharges during the wet season, with almost 125 mm of recharge in February (δS, Fig. 2a). Soil moisture is extracted at an average rate of 90 mm month^{-1} during the dry season (May–September), providing the moisture to meet evaporative demands. Simulated runoff remains low in the first half of the wet season (averaging less than 40 mm month^{-1} from October to February) but quickly increases to a peak value of 130 mm month^{-1} in April, when rainfall remains relatively high and soils are saturated (δS is near zero).

The simulated results are well-correlated with observation-based water balance estimates. Simulated ET has a strong positive bias (compared to MODIS), but the simulated and observed TWS and discharge are in excellent agreement. MODIS mean wet season ET (November–April) for the study period is 116 mm month^{-1}, ~16% less than IBIS mean wet season ET, while MODIS mean dry season ET (May–October) is 96 mm month^{-1}, ~20% less than the IBIS simulated dry season ET (Fig. 2a and b). GRACE and IBIS seasonal changes in water storage agree, with both estimating a mean wet season recharge of 90 mm month^{-1} and a dry season extraction of around 95 mm month^{-1} (Fig. 2a and b). There is a strong correlation in both the timing and magnitude of average monthly TWS anomalies (averaged over the XB from GRACE) and

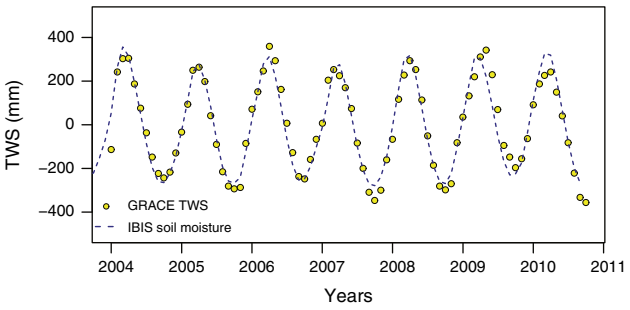

Fig. 3. Time series of TWS anomalies from GRACE and soil moisture anomalies from IBIS for Xingu River Basin.

IBIS-simulated anomalies in soil moisture storage ($r = 0.97$, $n = 81$) (Fig. 3). Soil moisture storage accounts for ~82% of IBIS simulated TWS change in the XB during the 2000s. This large soil moisture storage capacity and the movement of water through the soil column are reflected by a lag in the seasonal river flow, with lower discharge during the first half of the wet season (December–February) followed by increasing discharge in the subsequent months and dry season (Fig. 4). The simulated mean monthly discharge for the 2000s which included the MODIS land use and land cover information (RUN-LUC) also shows good agreement with observed mean monthly discharge measured at Altamira ($r = 0.90$, $n = 12$; Table 1). Observed and simulated runoff is low in the early wet season, peaking in April (114 and 130 mm month^{-1}, respectively) and tapering off slowly until September. From 2001 to 2010, the percent relative error of the simulated discharge was less than −5%, with IBIS underestimating discharge from December to January (compared to observed data) and overestimating it from March to May and into the dry season (Table 1).

3.1.3. Interannual variability

The interannual variability of the simulated and observed water balance components are correlated with precipitation, with some notable differences. For example, the interannual variability of the MOD16ET-derived water budget ($P - \mathrm{ET}_{\mathrm{MODIS}}$) correlates well with the observed discharge, but its magnitude is considerably greater (Fig. 4). The XB water balances derived from MOD16ET and IBIS-derived ET ($P - \mathrm{ET}_{\mathrm{MODIS}}$ and $P - \mathrm{ET}_{\mathrm{IBIS}}$ respectively) show very similar patterns ($r = 0.9$, $n = 10$), closely following annual precipitation but differing in magnitude (Fig. 4). Simulated ET had lower interannual variability than MOD16ET (Fig. 2a and b). Adding the monthly change in soil moisture storage (δS) to $P - \mathrm{ET}_{\mathrm{IBIS}}$ yields simulated discharge (R_{IBIS}), which also agrees well with observed discharge in terms of magnitude and interannual variability. Thus, although the net soil water storage is negligible over the long-term, short-term changes in soil moisture storage are responsible for considerable seasonal and annual variations in

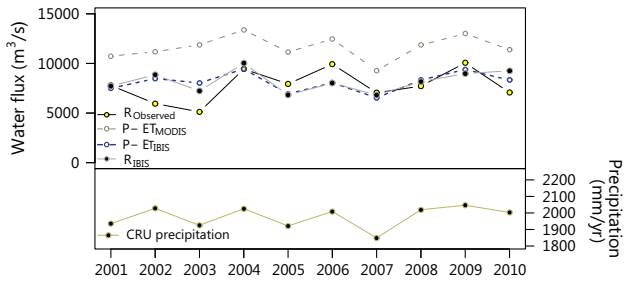

Fig. 4. Comparison of IBIS simulated discharge (R_{IBIS}) and calculated water balances (P – ET) to observed discharge (R_{Observed}) for Xingu River Basin.

discharge. Simulated discharge for the XB is very well-correlated with rainfall ($r = 0.87$, $n = 10$) over the study period.

3.2. Influence of land cover changes and climate on the XB hydrological budget

The strong agreement of simulated water budget components with those observed for the 2000s provides a baseline to analyze how and to what extent climate and historical deforestation are driving the variability in the water balance of the XB. In the following sections, we analyze the water balance changes that occurred in the XB from 1971 to 2010 and attribute them to climate variability, land cover changes, or both.

3.2.1. Changes in the water budget from the 1970s to the 2000s

An analysis of the individual components of change from the 1970s to the 2000s indicates that climate variability and land cover change have had opposite influences, with climate effects masking the changes due to historical deforestation (see Table 1). Precipitation decreased by 2% between the 1970s and 2000s (Table 1; not statistically significant, N.S.). Simulated ET and discharge registered small changes between the two decades (Table 1; +10 mm yr^{-1} and −48 mm yr^{-1}, respectively; N.S.). These small net changes in ET and discharge were the result of relatively large offsetting changes in annual rainfall (−2%, −48 mm yr^{-1}) and forest cover, which decreased from 90% to 75% of the Xingu Basin (around 100,000 km^2 deforested). The +10 mm yr^{-1} (+1%) increase in ET between decades was the net result of a +44 mm yr^{-1} increase from climate variations (RUN-POT) and a −34 mm yr^{-1} decrease from land cover changes. Similarly, a <1% net decrease (−14 mm yr^{-1}) in soil moisture was due to a −29 mm yr^{-1} decrease from climate variations and a +15 mm yr^{-1} increase from land cover change. The −48 mm yr^{-1} net decrease (−8%) in simulated discharge from the 1970s to the 2000s compares well with the observed −34 mm yr^{-1} decrease in discharge (−6%). Model simulations indicate that this net decrease in simulated discharge also resulted from competing factors, with climate variations causing a decrease of −82 mm yr^{-1} (−14%) and land cover changes causing an increase of +34 mm yr^{-1} (+6%).

3.2.2. Changes in water budget due to land cover changes in the 2000s

There was a modest change in the simulated XB water balance due to the decrease in forest cover from 80% of the basin in 2001 to 73% of the basin in 2010. Simulated evapotranspiration decreased by about ∼1%, average soil moisture increased by ∼0.1%, and discharge increased by +2% due to the prescribed land cover changes (Fig. 5). The annual decrease in percent forest cover from 2001 to 2010 was positively correlated to cumulative percent change in ET ($r = 0.99$, $n = 10$), and inversely correlated to cumulative percent change in soil moisture and discharge ($r = -0.98$, $n = 10$ in both instances). The shift from high deforestation rates prior to 2006 to the much lower rates after 2006 are reflected in the cumulative change in the water balance. Most of the cumulative change (∼80%) in the ET and discharge for the decade occurs in the period 2001–2006, with little change occurring after 2007 (Fig. 5).

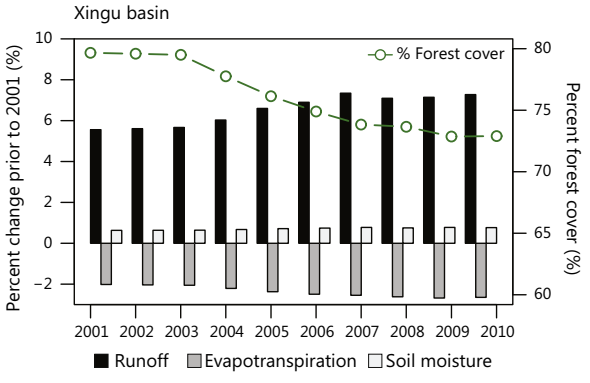

Fig. 5. Percent change in the simulated annual water balance components from 2001 to 2010 relative to the idealized potential vegetation simulation for Xingu Basin. The percent forest cover derived from MODIS land cover classification (green), ET (gray), soil moisture (white) and runoff (black). (For interpretation of the references to color in this figure legend, the reader is referred to the web version of this article.)

4. Discussion and conclusions

Overall, the IBIS-simulated water balance components show good seasonal and interannual agreement with satellite and field-based observations. Simulated ET seasonality for the 2001–2010 period is in good agreement with MOD16ET and ET inferred from observations (ET = P–R–δS). The magnitude of simulated ET is within ±5% of the observation-based ET estimates, which are about 20% greater than the MOD16 ET. Our results indicate that the MOD16 ET does not close the water balance (P–ET = R), which corroborates the findings of other studies in the US (Velpuri et al., 2013) and southern Brazil (Ruhoff et al., 2013). These studies suggest that the MOD16 algorithm may underestimate ET systematically, perhaps due to uncertainties inherent in the land cover classification map and other input datasets. IBIS simulated monthly changes in soil moisture storage ($\delta S/\delta t$) are comparable in magnitude and timing with the monthly GRACE TWS change (δTWS/δt). The remarkably good agreement between these two datasets suggests that a deep soil column (8-m in this study) is a necessary component for accurately modeling soil moisture dynamics in the Amazon. Finally, long-term observed discharge shows a net decrease of about −6% from the 1970s to the 2000s for the XB, which was reproduced well by IBIS when both climate and land cover change were included in the simulations.

Combining observed data, satellite products, and numerical modeling yielded insights into the Xingu water balance that would be difficult to achieve with any single method. For example, the deep soils of the XB and its highly seasonal and variable rainfall result in large seasonal fluctuations (∼500 mm) and interannual variability (∼100 mm) of water storage (Figs. 3 and 4). About 500 mm of excess rainfall is stored in the deep soil column during the wet season, which is then available to be extracted by evergreen forests in the dry season to meet high evaporative demand. This large soil water storage capacity plays a key role in forest maintenance during the long dry season of the southeastern Amazon.

Soil moisture storage may also drive some of the interannual variability observed in the discharge of the XB. For example, water years 2006, 2008, and 2009 had similar annual rainfall (about 2060 mm), but observed discharge in 2008 was about 500 mm, compared to 650 mm for 2006 and 660 mm for 2009 (Fig. 4). The runoff ratio (R/P) also dropped to 25% in 2008 from 30% in 2006 and 2009. This difference is likely because 2008 followed a very strong regional drought in 2007 (Brando et al., 2014). At the end of the 2007 dry season the observed TWS anomaly dropped to the second lowest level in the observational record. The total water storage change from the dry season low to the peak in 2008 was more than 100 mm greater than in 2006 and 2009 (Fig. 3), indicating that a relatively larger portion of the rainfall in 2008 went to replenishing soil moisture and less to discharge. In other parts of the Amazon (e.g. the NW Amazon), where the soils are almost continuously saturated, soil water storage anomalies are not a large contributor to TWS and discharge variation (Pokhrel et al., 2013).

Although soil moisture storage anomalies average to near zero over the long-term (decadal timescales), they can be large on shorter (interannual) timescales. Our results highlight the fact that these anomalies cannot be neglected when interpreting observations or simulating changes to the water balance in the XB and other regions with similar climatic and edaphic characteristics.

It is often impossible to evaluate the effect of land cover changes on different components of the water balance based on observations alone. In some cases the effects on the hydrological balance are too small to be detected (i.e. if the deforested area is relatively small), while in others climatic variability confounds the effects of land cover changes. The numerical model simulations in this study suggest that historical deforestation (1971–2010) and climate variability in the XB have each caused small changes in the water budget, but of opposite sign. Our results indicate that the −15% forest cover loss from the 1970s to the 2000s led to a −3% decrease in simulated ET, +1% increase in soil moisture, and +6% increase in simulated discharge for the XB. However, that change was masked by climatic variability that led to a −2% decrease in precipitation and a −14% decrease in discharge. Considered separately, land cover changes and climate variability have caused important changes from the 1970s to the 2000s, but because they are of opposite sign these are not evident in the few available long-term observation records (e.g. discharge).

Our analyses of observed and simulated data indicate that the XB has experienced only relatively small changes in the water cycle to date, and that protected areas have played an important role in limiting the direct impacts of deforestation. This study does not address changes to the water balance that could occur as a result of regional climate changes, either due to increasing atmospheric greenhouse gases or as a result of feedbacks from large-scale deforestation within or outside of the XB (Stickler et al., 2013). Such exogenously-driven climate changes appear to be small or undetectable with the current level of deforestation (Coe et al., 2013; Stickler et al., 2013) but could cause changes in the water balance in the coming decades comparable in scale to those directly due to land cover change, particularly in the southeastern Amazon (e.g. Coe et al., 2009, 2013; Malhi et al., 2008; Sampaio et al., 2007; Stickler et al., 2013).

Our results underscore the importance of public and private protected areas in regulating the water cycle of the Xingu Basin. Public protected areas, including a large mosaic of indigenous reserves, cover 55% of the XB. Together with forest set-asides on private properties required by the Brazilian Forest Code, protected forests have limited deforestation to less than 20% of the original forest cover in the XB, which explains the modest changes in the water cycle observed in this study. Our simulation results suggest that for every 1% decrease in forested area there is about a 2.1 mm yr^{-1} decrease in ET (Fig. 6) and a comparable increase in *R*. Under a constant climate, we expect that changes in the ET signal would exceed the background variability (twice the standard deviation) in ET once deforestation surpasses ~35% of the XB area (Fig. 6). Deforestation of either public or private protected areas in the Xingu could result in changes far exceeding this threshold. For example, if all protected forests on private lands were deforested (~45% of the basin area), there would be a −5% change in the simulated ET (Fig. 6) and a +13% increase in discharge. Complete deforestation of the XB would cause a −13% decrease in ET and a +32% increase in discharge. These results are consistent with observations in less protected and more heavily deforested watersheds. For example, more than 50% of the neighboring Araguaia River basin has been deforested, resulting in an ~18% increase in discharge (Coe et al., 2011). By contrast, the creation and maintenance of a mosaic of protected areas in the XB has played a significant role in buffering the region against similar changes to the water balance.

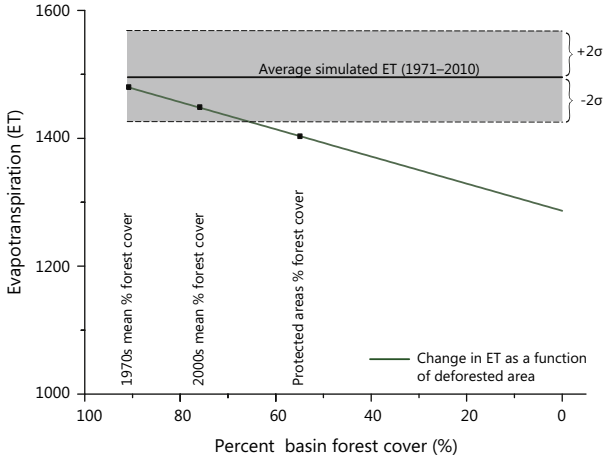

Fig. 6. Changes in IBIS-simulated ET (*y*-axis, mm/year) as a function of deforested area in the XB (*x*-axis, % forest cover). The 1971–2010 mean simulated ET (mm/year) for the potential vegetation run (RUN-POT, 90% forest cover) is shown as reference (solid black line), with the shaded area representing ±2 standard deviations (σ) from the mean. The mean simulated ET for the 1970s (90% forest) and 2000s (75% forest) decades are shown as solid black squares. The green line is a linear fit to the 1970s and 2000s. The final black square is the mean ET rate that would occur if all lands outside of protected areas were deforested (45% of basin remaining in forest). (For interpretation of the references to color in this figure legend, the reader is referred to the web version of this article.)

Although deforestation rates have decreased drastically in the last ten years (Macedo et al., 2012), significant pressures remain. Future climate projections predict a warmer climate, with increased probabilities of drought and wildfires (Alencar et al., 2011; Malhi et al., 2008; Nepstad et al., 2008), particularly in the eastern Amazon. Coupled with increasing demands for agricultural products (DeFries et al., 2013), future climate and land use changes are likely to increase pressure on existing forests. Policies and management strategies targeted at maintaining the physical integrity of protected areas, strengthening forest conservation on private properties, and preventing forest degradation will be critical to avoid large-scale disruptions of climate and ecosystem function in the region.

Acknowledgements

We would like to thank Pieter Beck and Divino Silvério for discussions helping data analyses. This work was supported through grants from the National Science Foundation (DEB0949996 and NSF-ICER 1343421), the National Aeronautic and Space Administration (NNX12AK11G), and the Gordon and Betty Moore Foundation.

References

Alencar, A., Asner, G.P., Knapp, D., Zarin, D., 2011. Temporal variability of forest fires in eastern Amazonia. Ecol. Appl. 21 (7), 2397–2412.
Barona, E., Ramankutty, N., Hyman, G., Coomes, O.T., 2010. The role of pasture and soybean in deforestation of the Brazilian Amazon. Environ. Res. Lett. 5 (2), 024002.
Bonan, G.B., 2008. Forests and climate change: forcings, feedbacks, and the climate benefits of forests. Science 320 (5882), 1444–1449.
Bosch, J.M., Hewlett, J., 1982. A review of catchment experiments to determine the effect of vegetation changes on water yield and evapotranspiration. J. Hydrol. 55 (1), 3–23.
Brando, P.M. et al., 2014. Abrupt increases in Amazonian tree mortality due to drought–fire interactions. Proc. Natl. Acad. Sci. 111 (17), 6347–6352.
Chen, J., Wilson, C., Tapley, B., Yang, Z., Niu, G., 2009. 2005 drought event in the Amazon River basin as measured by GRACE and estimated by climate models. J. Geophys. Res.: Solid Earth 114 (B5), 1978–2012.
Coe, M., Latrubesse, E., Ferreira, M., Amsler, M., 2011. The effects of deforestation and climate variability on the streamflow of the Araguaia River, Brazil. Biogeochemistry 105 (1–3), 119–131.

Coe, M.T., Costa, M.H., Soares-Filho, B.S., 2009. The influence of historical and potential future deforestation on the stream flow of the Amazon River-Land surface processes and atmospheric feedbacks. J. Hydrol. 369 (1), 165–174.
Coe, M.T. et al., 2013. Deforestation and climate feedbacks threaten the ecological integrity of south–southeastern Amazonia. Philos. Trans. R. Soc. B: Biol. Sci. 368 (1619).
Costa, M.H., Botta, A., Cardille, J.A., 2003. Effects of large-scale changes in land cover on the discharge of the Tocantins River, Southeastern Amazonia. J. Hydrol. 283 (1), 206–217.
Crowley, J.W., Mitrovica, J.X., Bailey, R.C., Tamisiea, M.E., Davis, J.L., 2008. Annual variations in water storage and precipitation in the Amazon Basin. J. Geodesy 82 (1), 9–13.
D'Almeida, C. et al., 2007. The effects of deforestation on the hydrological cycle in Amazonia: a review on scale and resolution. Int. J. Climatol. 27 (5), 633–647.
Davidson, E.A. et al., 2012. The Amazon basin in transition. Nature 481 (7381), 321–328.
de Linage, C., Famiglietti, J., Randerson, J., 2013. Forecasting terrestrial water storage changes in the Amazon Basin using Atlantic and Pacific sea surface temperatures. Hydrol. Earth Syst. Sci. Discuss. 10 (10).
De Moraes, J.M., Schuler, A.E., Dunne, T., Figueiredo, R.D.O., Victoria, R.L., 2006. Water storage and runoff processes in plinthic soils under forest and pasture in eastern Amazonia. Hydrol. Process. 20 (12), 2509–2526.
DeFries, R., Herold, M., Verchot, L., Macedo, M.N., Shimabukuro, Y., 2013. Export-oriented deforestation in Mato Grosso: harbinger or exception for other tropical forests? Philos. Trans. R. Soc. B: Biol. Sci. 368 (1619), 20120173.
Foley, J.A. et al., 2005. Global consequences of land use. Science 309 (5734), 570–574.
Foley, J.A. et al., 1996. An integrated biosphere model of land surface processes, terrestrial carbon balance, and vegetation dynamics. Global Biogeochem. Cycles 10 (4), 603–628.
Hayhoe, S.J. et al., 2011. Conversion to soy on the Amazonian agricultural frontier increases streamflow without affecting stormflow dynamics. Glob. Change Biol. 17 (5), 1821–1833.
Hodnett, M., da Silva, L.P., Da Rocha, H., Cruz Senna, R., 1995. Seasonal soil water storage changes beneath central Amazonian rainforest and pasture. J. Hydrol. 170 (1), 233–254.
Kucharik, C.J. et al., 2000. Testing the performance of a dynamic global ecosystem model: water balance, carbon balance, and vegetation structure. Global Biogeochem. Cycles 14 (3), 795–825.
Landerer, F., Swenson, S., 2012. Accuracy of scaled GRACE terrestrial water storage estimates. Water Resour. Res. 48 (4).
Lathuillière, M.J., Johnson, M.S., Donner, S.D., 2012. Water use by terrestrial ecosystems: temporal variability in rainforest and agricultural contributions to evapotranspiration in Mato Grosso, Brazil. Environ. Res. Lett. 7 (2), 024024.
Li, K., De Jong, R., Coe, M., Ramankutty, N., 2006. Root-water-uptake based upon a new water stress reduction and an asymptotic root distribution function. Earth Interact. 10 (14), 1–22.
Macedo, M.N. et al., 2013. Land-use-driven stream warming in southeastern Amazonia. Philos. Trans. R. Soc. B: Biol. Sci. 368 (1619).
Macedo, M.N. et al., 2012. Decoupling of deforestation and soy production in the southern Amazon during the late 2000s. Proc. Natl. Acad. Sci. 109 (4), 1341–1346.
Malhi, Y. et al., 2008. Climate change, deforestation, and the fate of the Amazon. Science 319 (5860), 169–172.
Mu, Q., Heinsch, F.A., Zhao, M., Running, S.W., 2007. Development of a global evapotranspiration algorithm based on MODIS and global meteorology data. Remote Sens. Environ. 111 (4), 519–536.
Mu, Q., Zhao, M., Running, S.W., 2011. Improvements to a MODIS global terrestrial evapotranspiration algorithm. Remote Sens. Environ. 115 (8), 1781–1800.
Neill, C. et al., 2013. Watershed responses to Amazon soya bean cropland expansion and intensification. Philos. Trans. R. Soc. B: Biol. Sci. 368 (1619).
Neill, C. et al., 2006. Hydrological and biogeochemical processes in a changing Amazon: results from small watershed studies and the large-scale biosphere-atmosphere experiment. Hydrol. Process. 20 (12), 2467–2476.
Nepstad, D. et al., 2009. The end of deforestation in the Brazilian Amazon. Science 326 (5958), 1350–1351.
Nepstad, D.C. et al., 1994. The role of deep roots in the hydrological and carbon cycles of Amazonian forests and pastures. Nature 372, 666–669.
Nepstad, D.C., Stickler, C.M., Almeida, O.T., 2006. Globalization of the Amazon soy and beef industries: opportunities for conservation. Conserv. Biol. 20 (6), 1595–1603.
Nepstad, D.C., Stickler, C.M., Soares-Filho, B., Merry, F., 2008. Interactions among Amazon land use, forests and climate: prospects for a near-term forest tipping point. Philos. Trans. R. Soc. B: Biol. Sci. 363 (1498), 1737–1746.
Pokhrel, Y.N., Fan, Y., Miguez-Macho, G., Yeh, P.J.F., Han, S.C., 2013. The role of groundwater in the Amazon water cycle: 3. influence on terrestrial water storage computations and comparison with GRACE. J. Geophys. Res.: Atmos. 118 (8), 3233–3244.
Pongratz, J. et al., 2006. The impact of land cover change on surface energy and water balance in Mato Grosso, Brazil. Earth Interact. 10 (19), 1–17.
Ramankutty, N., Foley, J.A., 1998. Characterizing patterns of global land use: an analysis of global croplands data. Global Biogeochem. Cycles 12 (4), 667–685.
Rodell, M. et al., 2004. Basin scale estimates of evapotranspiration using GRACE and other observations. Geophys. Res. Lett. 31 (20).
Ruhoff, A. et al., 2013. Assessment of the MODIS global evapotranspiration algorithm using eddy covariance measurements and hydrological modelling in the Rio Grande basin. Hydrol. Sci. J. 58 (8), 1658–1676.
Sampaio, G. et al., 2007. Regional climate change over eastern Amazonia caused by pasture and soybean cropland expansion. Geophys. Res. Lett. 34 (17).
Scanlon, B.R., Jolly, I., Sophocleous, M., Zhang, L., 2007. Global impacts of conversions from natural to agricultural ecosystems on water resources: quantity versus quality. Water Resour. Res. 43 (3).
Schwartzman, S. et al., 2013. The natural and social history of the indigenous lands and protected areas corridor of the Xingu River basin. Philos. Trans. R. Soc. B: Biol. Sci. 368 (1619), 20120164.
Silvério, D. Agricultural expansion reduces net radiation and shifts energy partitioning in tropical forests. Environmental Research Letters (Submitted for publication).
Stickler, C.M. et al., 2013. Dependence of hydropower energy generation on forests in the Amazon Basin at local and regional scales. Proc. Natl. Acad. Sci. 110 (23), 9601–9606.
Swenson, S., Wahr, J., Milly, P., 2003. Estimated accuracies of regional water storage variations inferred from the gravity recovery and climate experiment (GRACE). Water Resour. Res. 39 (8).
Velpuri, N., Senay, G., Singh, R., Bohms, S., Verdin, J., 2013. A comprehensive evaluation of two MODIS evapotranspiration products over the conterminous United States: using point and gridded FLUXNET and water balance ET. Remote Sens. Environ. 139, 35–49.
Williams, M.R., Melack, J.M., 1997. Effects of prescribed burning and drought on the solute chemistry of mixed-conifer forest streams of the Sierra Nevada, California. Biogeochemistry 39 (3), 225–253.